Investigation of the Factors Affecting Surface-Plasmon Efficiency

Padmarekha Vemuri, University of North Texas; Vijay Vaidyanathan, University of North Texas; Arup Neogi, University of North Texas

Abstract

Group-III nitride-based semiconductors have emerged as the leading material for short wavelength optoelectronic devices. The gallium nitride/indium-gallium nitride (GaN/InGaN) alloy system forms a continuous and direct bandgap semiconductor spanning ultraviolet (UV) to blue/green wavelengths. An ideal and highly efficient light-emitting device can be designed by enhancing the spontaneous emission rate. The paper presents the design and fabrication of a visible-light-emitting device using a GaN/InGaN single-quantum-well system with enhanced spontaneous emission. To increase the emission efficiency, layers of different metals, usually noble metals like silver, gold and aluminum, were deposited on GaN/InGaN single-quantum-wells using a metal evaporator. Surface characterization of metal-coated GaN/InGaN single-quantum-well samples was carried out using Atomic Force Microscopy (AFM) and Scanning Electron Microscopy (SEM). Photoluminescence (PL) was used as a tool for optical characterization to study the enhancement in the light emitting structures. This study also compared characteristics of different metals on GaN/InGaN single-quantum-well systems, thus allowing selection of the most appropriate material for a particular application. Results show that photons from the light emitter couple more to the surface plasmons if the band-gap of the former is close to the surface-plasmon resonant energy of a particular metal. Absorption of light due to gold reduces the effective mean path of light emitted from the light emitter and hence quenches the quantum-well emission peak compared to the uncoated sample.

Introduction

Semiconductor materials play a vital role both in optoelectronics and high-speed digital circuits for computer and telecommunication applications. Silicon semiconductor technology has advanced exponentially in both performance and productivity as predicted by Moore's law [1]. These exponential advances in device integration observed over the past several decades might soon end due to fundamental physical (lithographic area not less than 100nm) and/or economic (cost of fabrication facility more than US $2 billion) limitations [2]. The 1999 edition of the *International Technology Roadmap for Semiconductors* reported the presence of a potential "Red Brick Wall" that could block further scaling of integrated circuits [3].

This prediction has motivated extensive efforts aimed at developing new device concepts and fabrication approaches that may enable integration to overcome the limits of conventional microelectronics technology [2]. It requires the development of an optical analogue of an electronic integrated circuit capable of routing, controlling and processing optical signals [4]. There is a strong tendency to replace big and slow electronic devices with small and fast photonic ones. Development of photonic crystals, quantum wells, and quantum dots, having key properties controlled by size, morphology, and chemical composition, represents a powerful approach that could overcome physical and/or economic limitations [2]. The photonic integrated circuit include devices such as switches, sources and interconnects to accommodate 1000 x 1000 channels on a single substrate [5]. A novel nanophotonic technology that goes beyond the diffraction limit is essential to meet the demands of the future semiconductor optoelectronic industry. Surface plasmons are an integral part of nanophotonic technology that could potentially fill a niche in the optoelectronics industry.

Surface Plasmons

Surface plasmons are trapped electromagnetic surface modes at the interface between a metal and a dielectric and are a combined oscillation of the electromagnetic field and the surface charges of the metal [6]. They are widely recognized in the field of surface science. Surface plasmons have electromagnetic fields that decay exponentially into both the metal and dielectric media that bound the interface [7]. Surface plasmons propagate along an interface between two media with dielectric constants of opposite sign (such as a metal and a dielectric). Renewed interest in surface plasmons comes from recent advances that allow metals to be structured and enable concentration and channeling of light using sub-wavelength structures. This in turn facilitates control of surface-plasmon properties to reveal new aspects of their underlying science and to tailor them for specific applications [7].

The use of surface plasmons to concentrate light in sub-wavelength structures stems from the different permittivity, (ε), of the metals and the surrounding non-conducting media. In order to sustain surface-plasmon resonance, the metal concerned must have conduction-band electrons capable of resonating with light of the appropriate wavelength. Surface plasmons of lower frequency, ω_{sp} , can also be excited by high-energy electron beams or by light. Thus, using surface

plasmons that are trapped at the interface, the problem of light manipulation can be simplified from three dimensions to two dimensions [8]. Surface plasmons can increase the density of states (energy levels) and the spontaneous emission rate in the semiconductor, and lead to the enhancement of light emission by surface-plasmon quantum-well coupling [9], [10].

In order to build an ideal and highly-efficient light-emitting device, it is desirable to enhance the spontaneous emission rate. Coupling the light to the surface plasmons of a metallic film can enhance spontaneous emission and thereby optical emission of the semiconductor. Metal-semiconductor surface-plasmon interaction is an effective tool for manipulating local interaction for various optoelectronic applications [11]. The purpose of this study was to design and fabricate a visible-light-emitting device using the GaN/InGaN single-quantum-well system with enhanced spontaneous emission. To increase the emission efficiency, layers of different metals, usually noble metals like silver (Ag), gold (Au) and aluminum (Al), were deposited on the GaN/InGaN single-quantum-wells using a metal evaporator. The bottom surfaces of the single-quantum-well samples (sapphire substrate) were polished to avoid scattering of light. Surface characterization of metal-coated GaN/InGaN single-quantum-well samples was carried out using Atomic Force Microscopy (AFM) and Scanning Electron Microscopy (SEM). Photoluminescence (PL) was used as a tool for optical characterization to study the enhancement of light-emitting structures. This study also compared characteristics of different metals on the GaN/InGaN single-quantum-well systems, thus allowing selection of the most appropriate material for a particular application.

Methods

The experimental procedure was divided into two sections, deposition and characterization. The first section involved deposition of thin metal films on the GaN/InGaN single-quantum-wells in an ultra-high vacuum chamber by using a metal evaporator, while the second section dealt with characterization of the metal-coated GaN/InGaN single-quantum-wells.

GaN/InGaN Single-Quantum-Wells

Three GaN/InGaN samples (growth temperatures: 780°, 800°, and 830°C) were grown at the Institute of Photonics, University of Strathclyde, Glasgow, Scotland, U.K (collaboration). Metal organic-chemical vapor deposition or metal organic-vapor phase epitaxy was used to grow epitaxial structures of samples by depositing atoms on a sapphire substrate. Ammonia (NH_3) was used as a precursor for nitrogen, whereas trimethygallium and trimethylindium were used as gallium and indium sources, respectively. Typically, the growth rate employed was one to three mono-layers per second, approximately 0.3-1μm/hr, although much higher growth rates can be attained. Compounds were grown in a hydrogen atmosphere where they formed epitaxial layers on the substrate as they decomposed [12]. In order to study the enhancement in light emission from metal-coated GaN/InGaN single-quantum-well samples, the samples needed to be excited from the bottom surface. Rough bottom surfaces scatter the light and drop the efficiency of light reaching the quantum wells. Hence the substrate side (bottom surface) of the samples had to be polished. Mechanical polishing is commonly used to smooth surfaces [13]. An Allied Tech Prep™ P/N 15-2000 mechanical polisher was used to polish the samples used in this study.

Sample Preparation

Samples used for metal deposition and further characterization were cleaned thoroughly for best results. The three different GaN/InGaN single-quantum-well samples were cut into four pieces each for metal deposition. The protocol for cleaning the GaN/InGaN samples is as follows:

- Rinse the samples in acetone for 5 minutes.
- Clean the samples in distilled water 2 to 3 times.
- Rinse the samples in methanol for 3 minutes.
- Clean the samples with distilled water again, 2 to 3 times.
- Place the samples in 15% ($HCl+HNO_3$) Aqua Regia solution and heat the solution to approximately 80°C.
- Clean the samples with distilled water 4 times.
- Blow-dry the samples with dry nitrogen gas.

Thickness Monitoring

A Maxtek TM-100 Thickness Monitor was used to monitor the thickness of the metal films during the deposition process. The thickness monitor allows improved manual control of the vacuum film deposition process by providing a direct display of film thickness and deposition rate during deposition.

Thin-Film Characterization

Physical and optical analyses were carried out on all the metal-deposited single-quantum-well samples. Scanning Electron Microscopy (SEM) was performed using the JEOL-5800™ SEM. All samples with and without metal films deposited were physically examined under the SEM to understand their surface morphology. Atomic Force Microscopy (AFM) was used to make a physical analysis. Digital In-

strument's Nanoscope-E® AFM was used in this study. A photoluminescence technique was used to perform optical analysis. Figure 1 shows the photoluminescence arrangement with a system made up of a laser (light source), lenses and spectrometer interfaced to a PC.

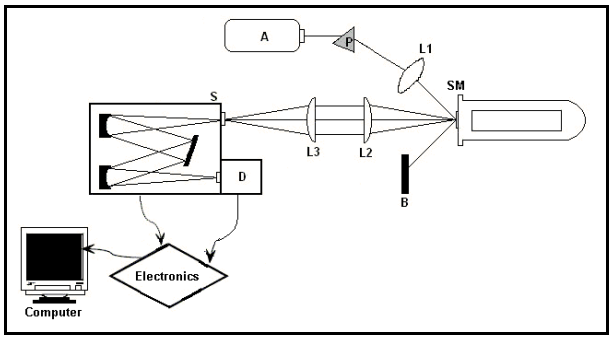

Figure 1: Simplified Photoluminescence arrangement, with Laser (A), Lenses (L1, L2, L3), Prism (P), Beam block (B), Sample (SM) inside Cryostat (C), Spectrometer (S), and Detector (D)

The enhancement of optical emission induced by surface-plasmon interaction was studied by using a two-dimensional emitter situated within the surface-plasmon penetration depth of the semiconductor light-emitting structure. For the development of efficient light emitters, the quantum-well widths were varied by growing the samples at different temperatures. Three GaN/InGaN quantum-well samples were grown with varying quantum-well widths for achieving varying emission energies. Sample preparation was carried out by first polishing the bottom surface of sapphire substrate grown, single-quantum-well samples and later by cleaning the samples for metal deposition. Thin metal (Ag/Au/Al) films were deposited using a metal evaporator.

The quantum-well samples were characterized for surface roughness using SEM and AFM. The enhancement in light emission was investigated using Photoluminescence (PL) spectroscopy. A GaN buffer layer of approximately 1.5μm thick was deposited on the sapphire substrate. Single InGaN quantum wells were grown on the GaN buffer layer at various temperatures measured by a pyrometer within the growth chamber. The growth run was finished by a GaN cap layer of 17nm thickness, grown at the same temperature as the InGaN quantum wells. The growth time for the cap was held at 36 s, with the GaN growth rate only slightly dependent on temperature over the range concerned. Table 1 represents the classification of samples based on their quantum-well (QW) emission and growth temperatures.

Sample A was grown at 780˚C with a well thickness of 4.05nm. Sample B was grown at 800˚C with a well thickness of 4.3nm. Similarly, Sample C was grown at 830˚C and has a well thickness of 4.55nm. Each sample was cut into four pieces and Ag/Au/Al metal films were deposited.

Table 1: Sample Classification

Sample Name	QW Energy (eV)	QW Thickness	Growth Temperature	Metal Deposited
Sample A-No Metal	2.53	4.05nm	830℃	None
Sample A-Silver	2.53	4.05nm	830℃	Silver
Sample A-Gold	2.53	4.05nm	830℃	Gold
Sample A-Aluminum	2.53	4.05nm	830℃	Aluminum
Sample B-No Metal	2.25	4.3nm	800℃	None
Sample B-Silver	2.25	4.3nm	800℃	Silver
Sample B-Gold	2.25	4.3nm	800℃	Gold
Sample B-Aluminum	2.25	4.3nm	800℃	Aluminum
Sample C-No Metal	2.1	4.55nm	780℃	None
Sample C-Silver	2.1	4.55nm	780℃	Silver
Sample C-Gold	2.1	4.55nm	780℃	Gold
Sample C-Aluminum	2.1	4.55nm	780℃	Aluminum

Results and Discussion

a) Surface Characterization

Scanning Electron Microscopy did not show significant quantitative roughness. Hence, AFM characterization was carried out on uncoated and metal-coated samples to determine the surface roughness. A scan size of 6μm x 6μm and a scan rate of 5.0Hz were used to scan the samples. The GaN domains of 1μm x 1μm (approximately) were observed on Sample A-No Metal, which are not periodic and, an average roughness of ~ 1nm was observed over a range of 6μm x 6μm of the scanned area. Due to the existence of domains on the GaN surface, some domains were observed on the silver-coated surface. These domains contribute to the roughness in the silver-coated sample. For gold-coated samples, a sample roughness of ~2.5nm was observed. Cluster formation was observed on both the gold and aluminum-coated samples of Sample A. From the images of AFM on Sample A, it was observed that the samples have an average roughness of approximately 1 to 2nm and do not have any periodic roughness.

An AFM characterization on Sample B was carried out on both the uncoated and metal-coated samples in order to determine the surface roughness. Based on the study of AFM images, it was observed that the samples had an average roughness of approximately 1 to 2nm and did not have any periodic roughness. Cluster formation was observed on gold- and aluminum-coated samples. From the images of AFM on Sample C, it was observed that the samples had an average

roughness of approximately 2 to 3nm and did not have any periodic roughness.

b) Photoluminescence Characterization

In the front incidence and front collection geometry as discussed earlier, photoluminescence (PL) characterization on the samples was conducted using an excitation of a 325 nm line of the He-Cd laser, operated at < 22.5mW, and detected using a charge-coupled device (CCD) array. Figure 2 shows the PL spectrum of Sample A at room temperature (300K). The peak at 360 nm corresponds to the emission peak, mostly from the GaN cap layer and partially from the GaN buffer layer. The peak at 495 nm corresponds to the quantum-well emission at room temperature. The small broad peaks from 400 to 475 nm are identified as optically-deep-level transition peaks from GaN cap/buffer layers. An increase in the intensity of emission from both quantum-well and GaN (cap/buffer) layers was observed from the spectrum at low temperatures.

Figure 3 shows the PL spectrum of Sample B at room temperature (300K). The peak at 360nm corresponds to the emission peak, mostly from the GaN cap layer and partially from the GaN buffer layer. The peak at 544nm corresponds to the quantum-well emission at room temperature. An increase in the intensity of emission from both quantum-well and GaN (cap/buffer) layers was observed from the spectrum at low temperatures. The PL intensity peak was observed at a wavelength of 550 nm.

Figure 4 shows the PL spectrum of Sample C at room temperature (300K). The peak at 360nm corresponds to the emission peak, mostly from the GaN cap layer and partially from the GaN buffer layer. The peak at ~585nm corresponds to the quantum-well emission at room temperature. An increase in the intensity of emission from both QW and GaN (cap/buffer) layers was observed from the spectrum at low temperatures. At low temperatures, the intensity peak was observed at 595 nm.

Non-radiative recombination of the electron-hole pairs in the light emitters dominates at room temperature due to phonons being produced instead of photons. Hence, the intensity

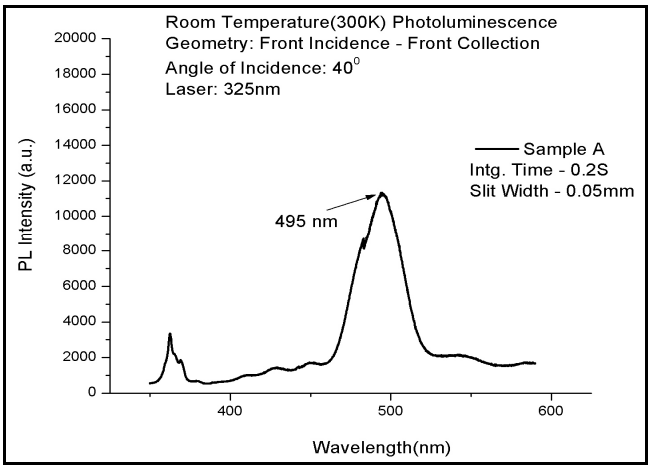

Figure 2: Room Temperature PL of Sample A

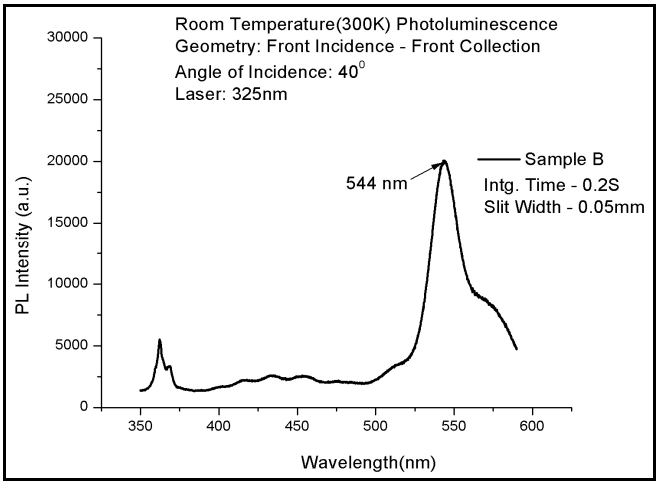

Figure 3: Room Temperature PL of Sample B

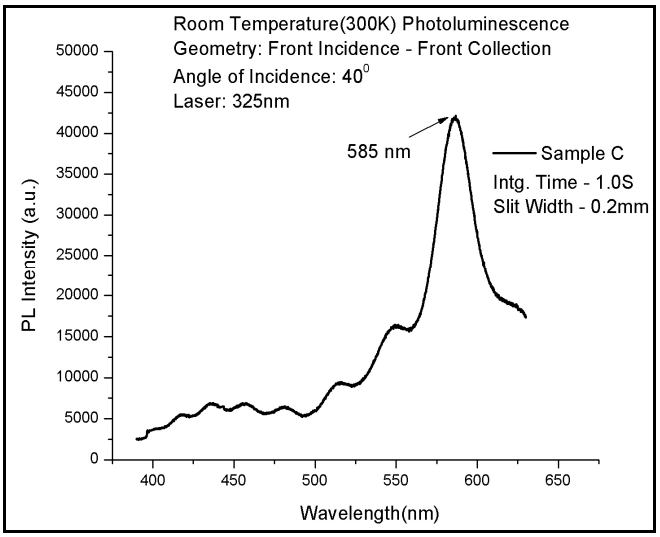

Figure 4: Room Temperature PL of Sample C

drops. At low temperatures, the electrons recombine with holes in a radiative recombination process releasing more photons, resulting in higher intensity.

c) Angle-Resolved PL Spectroscopy in the Backscattered Geometries

The metal-coated samples were photo-excited at 35˚, 40˚, 45˚, 50˚, and 55˚ angle of incidence and PL was measured from the back of the unpolished sapphire substrate. Reflection from the metal films on the front side of the sample restricts the use of front-incidence, front-collection geometry. When exciting the quantum well from the backside of the sample, the 325nm (~3.8eV) He-Cd laser cannot be used since the laser light is absorbed mostly by the bulk GaN buffer layer (emission energy ~3.4eV). Thus, not enough photons reach the quantum-well layer to excite the electron-hole recombination. Therefore, a 405nm (~2.8eV) diode laser was used in the back-incidence, back-collection geometry. In this geometry, GaN is transparent to the incident light and, hence, maximum light reaches the quantum well. Scattering was observed on the uncoated gold- and aluminum-coated samples of Sample A. A peak at 490 nm was observed only on silver-coated samples (Sample A-Silver) at all angles of incidence. A statistical analysis using a T-test was carried out to decide whether there is a significant change in the PL intensities from polished and unpolished samples.

With μ_p being the mean of peak PL intensities from polished Sample A-silver and μ_{up} being the mean of peak PL intensities from unpolished Sample A-silver, the null and alternate hypothesis can be stated as follows:

Null Hypothesis H_0: There is no significant change in peak PL intensity from unpolished and polished samples at all angles of incidence.

$$H_0: \mu_p = \mu_{up}$$

Research Hypothesis (Alternate Hypothesis) H_1: There is a significant change in peak PL intensity from unpolished and polished samples at all angles of incidence.

$$H_1: \mu_p \neq \mu_{up}$$

Test Statistic: The statistical T-test of "Paired Two Sample for Means" created using Microsoft Excel is shown in Table 2 [16]. This test was conducted on the data with a confidence coefficient (α) of 0.05 to test the equality of means of peak PL intensities from polished and unpolished samples.

Since $|T_{stat}| > T_{critical\ two\text{-}tail}$, the decision rule is to reject the null hypothesis and, hence, accept the Alternate Hypothesis (H_1). This implies that there is a significant difference (significance level, $\alpha = 0.05$) in the mean peak PL intensities between unpolished and polished samples. Thus, it can be inferred that polishing is required to avoid scattering and enhance the light emission from quantum wells.

d) PL Spectroscopy

The variation of peak photoluminescence intensity with angle of incidence for sample A is shown in Figure 5. No enhancement was observed in the gold-coated sample. Similar plots for sample B and sample C are shown in Figure 6 and Figure 7, respectively.

Table 2: T-Test on Peak PL Intensity from Polished and Unpolished Samples

T-Test: Paired Two Sample for Means		
	Unpolished Sample A-Silver	*Polished Sample A-Silver*
Mean	14588.88588	47523.21135
Variance	1970594.689	50934464.45
Observations	5	
Pearson Correlation	-0.986459103	
Hypothesized Mean Difference	0	
Df	3	
T Stat	-7.726783237	
P(T<=t) two-tail	0.004507007	
T Critical two-tail	3.182449291	

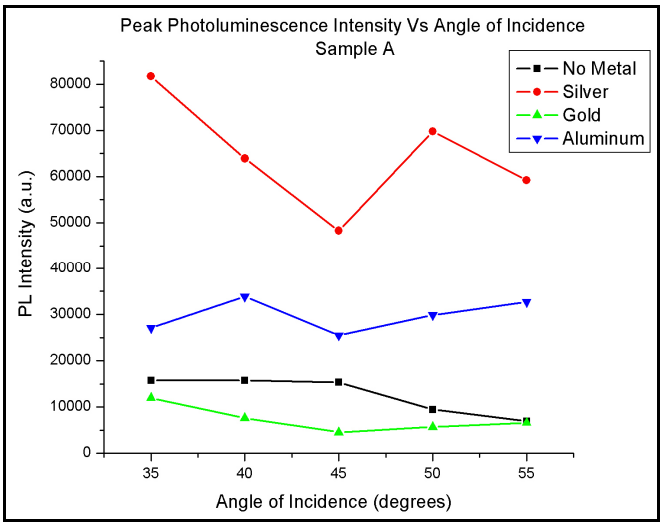

Figure 5: Peak PL intensity of Sample A versus Angle of Incidence

The PL enhancement after coating the samples (Sample A, Sample B with different metals) is attributed to the strong interaction with surface plasmons. Electron hole pairs excited in the quantum well couple to the surface plasmons at the GaN/Metal interface when the energies of the electron-hole

pairs in InGaN ($\hbar\omega_{InGaN}$) and of metal surface plasmons ($\hbar\omega_{SP}$) are similar. Then, electron-hole recombination produces surface plasmons instead of photons and this new recombination path increases the spontaneous recombination rate. According to the condition for surface-plasmon coupling:

$$\hbar\omega_{SP} \geq \hbar\omega_{InGaN}$$

For silver, $\hbar\omega_{SP} > \hbar\omega_{InGaN}$, hence the electron-hole pairs excited in Sample-A and Sample-B couple to the

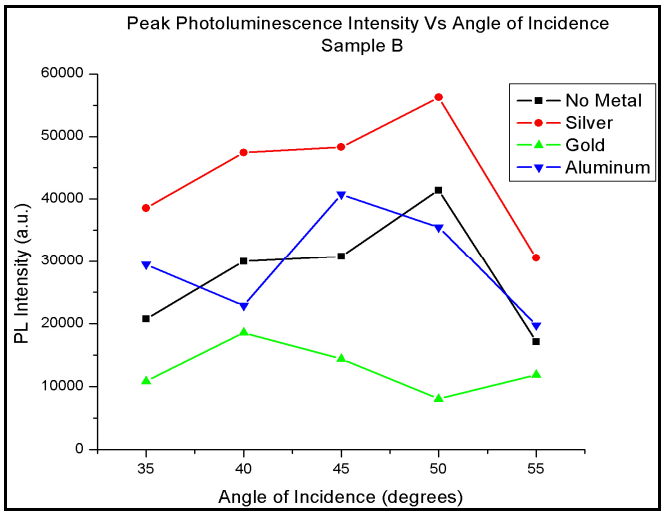

Figure 6: Peak PL intensity of Sample B versus Angle of Incidence

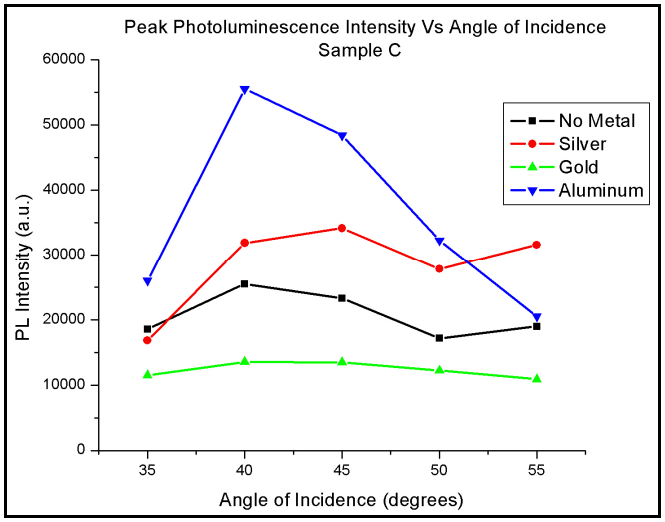

Figure 7: Peak PL intensity of Sample C versus Angle of Incidence

surface plasmons at the GaN/Ag interface. Surface plasmons increase the density of states and, in turn, increase the spontaneous-emission recombination rate. Hence, more electrons recombine with holes to produce more photons. The resulting enhancement was observed in the silver-coated samples.

In the case of aluminum-coated samples of both Sample-A and Sample-B, $\hbar\omega_{SP} >> \hbar\omega_{InGaN}$, hence the electron-hole pairs couple to the surface plasmons at the GaN/Al interface. The real part of the dielectric constant of aluminum is negative over a wide wavelength region for visible light. Thus, an increase in PL intensity was observed on the aluminum-coated samples. For the gold-coated samples, $\hbar\omega_{SP} < \hbar\omega_{InGaN}$. This does not satisfy the condition for surface-plasmon coupling. Therefore, no enhancement was observed in the gold-coated samples.

Tuning the angle of incidence or polarization of excitation light can effectively excite surface plasmons. In general, surface plasmons cannot be excited on flat metallic film by electromagnetic radiation with optical frequencies since light does not have enough momentum (k_{ph}) to excite a surface plasmon with momentum k_{sp}. The photons can obtain additional momentum ($k_{roughness}$) via the roughness or defects on the sample surface.

Hence: $\boldsymbol{k_{SP} = k_{ph} + k_{roughness}}$

$$= \frac{\omega}{c} \times \sin\theta + k_{roughness}$$

where ω is the excitation photon frequency in s^{-1},
θ is the angle from the surface normal to the incoming photon direction (angle of incidence) in degrees, and
c is speed of light in nm/s^2

Surface plasmons can be excited only when momentum conservation is fulfilled. With ω and c being constant, momentum conservation can be achieved by rotating either the sample with respect to the excitation beam or by introducing periodic roughness, i.e., by fabricating periodic corrugations. In the present set up, the excitation beam was rotated with respect to the stationary sample. In Sample A, an increase in the PL peak intensity was observed from the silver-coated sample when compared to the uncoated sample at all incident angles. The drop in the peak PL intensity in the silver-coated sample at a 45˚ angle of incidence can be attributed to the roughness and non-uniformity of the sample surface. An enhancement in the peak PL intensity from the aluminum-coated sample was observed at all angles of incidence when compared to the uncoated sample and no enhancement was observed in the gold-coated samples. For Sample B, an increase in the PL peak intensity from 35° to 50° angles of incidence was observed in both silver-coated and uncoated samples. No particular trend was observed in the aluminum-coated sample. A drop in PL intensity was observed from the gold-coated samples at all angles of incidence.

Compared to Samples A and B, the enhancement in the peak PL intensity observed in the silver-coated Sample C was not as high. Also, a drop in the peak PL intensity was

observed in the gold-coated samples (Sample C-Gold). The reduction in the PL enhancement ratio could be due to the higher plasmon energy of silver compared to the quantum-well energy, which leads to a mismatch in the energies. Inefficient resonant plasmon coupling occurs due to the energy mismatch, which leads to a reduced spontaneous emission rate. The PL enhancement after coating the quantum-well samples of Sample C with different metals is attributed to the strong interaction with surface plasmons.

According to the condition for surface-plasmon coupling:

$$\hbar\omega_{SP} \geq \hbar\omega_{InGaN}$$

For silver, $\hbar\omega_{SP} > \hbar\omega_{InGaN}$, hence the electron-hole pairs excited in Sample C should couple to the surface plasmons at the GaN/Ag interface. The quantum-well energy is much smaller than the plasmon energy resulting in weak coupling and, in turn, lower enhancement was observed. Part of the enhancement in the PL can also be attributed to the reflection of pump light at the silver/GaN interface. In the case of the aluminum-coated samples, $\hbar\omega_{SP} >> \hbar\omega_{InGaN}$, hence the electron-hole pairs couple to the surface plasmons at the GaN/Al interface. Also, the sub-wavelength roughness on the sample surface helps to effectively excite the surface plasmons. Some enhancement in the PL intensity can be attributed to the reflection of pump light at the GaN/Al interface back through the quantum well. Thus, an increase in PL intensity was observed on the aluminum-coated samples. In the case of the gold-coated samples, even though $\hbar\omega_{SP} > \hbar\omega_{InGaN}$, the high absorption of gold in the visible region is responsible for no enhancement. The pump light and the light emitted by the light emitter are absorbed by the gold film, which leads to quenching of the quantum-well peak.

e) Statistical Analysis

An analysis of Variance (ANOVA) was performed to determine the effect of different metals at different angles of incidence on each sample. In the ANOVA, a comparison was made between three or more population means to determine whether they could be equal [16]. With μ_{metal} being the mean of the peak PL intensities from different metal-coated and uncoated samples, and μ_{angle} being the angle of incidence, the null and alternate hypotheses can be stated as follows:

Null Hypothesis (H_n): There are two variables (Columns and Rows) based on which hypothesis written and ANOVA analysis is performed.
Rows: There is no significant variation in the mean peak PL intensities due to different angles of incidence.

Columns: There is a no significant variation in the mean peak PL intensities due to different metal coatings on samples.

$$H_{n1}: \mu_{35} = \mu_{40} = \mu_{45} = \mu_{50} = \mu_{55}$$
$$H_{n2}: \mu_{Ag} = \mu_{Au} = \mu_{Al} = \mu_{uncoated}$$

Alternate Hypothesis (H_a):
Rows: There is a significant variation in the mean peak PL intensities due to different angles of incidence.

Columns: There is a significant variation in the mean peak PL intensities due to different metal coatings on sample.

H_{a1}: At least two of μ_{35}, μ_{40}, $\mu_{45,}$ μ_{50} and $\mu_{55,}$ differ.
H_{a2}: At least two of μ_{Ag}, μ_{Au}, μ_{Al} and $\mu_{uncoated}$ differ.

ANOVA on Sample A:

The peak PL intensities at all angles of incidence from uncoated and metal-coated samples of Sample A were tabulated for statistical analysis. Using Microsoft Excel, a "Two-Way ANOVA Without replication" was performed to either accept or reject the null hypothesis. The results of the ANOVA analysis are shown in Table 3.

Since $|F_{Calculated}|$ (Rows) < $F_{critical}$ (Rows), the decision rule is that we fail to reject the null hypothesis (H_{n1}) and, hence, accept the null hypothesis (H_{n1}). This implies that there is no significant difference (significance level, $\alpha = 0.05$) in the mean peak PL intensities due to a change in the angle of incidence in Sample A.

Since $|F_{Calculated}|$ (Columns) > $F_{critical}$ (Columns), the decision rule is to reject the null hypothesis (H_{n2}) and, hence, accept the alternate hypothesis (H_{a2}). This implies that there is a significant difference (significance level, $\alpha = 0.05$) in the mean peak PL intensities due to different metal coatings on Sample A.

Table 3: ANOVA of Sample A

Source of Variation	*SS*	*Degree of Freedom*	*MS*	*F*	*F crit*
Rows	261244655.5	4	65311163.88	1.540945367	3.259160053
Columns	10042560323	3	3347520108	78.98106991	3.490299605
Error	508605939.9	12	42383828.32		
Total	10812410919	19			

ANOVA on Sample B:

The peak PL intensities at all angles of incidence from the uncoated and metal-coated samples of Sample B were tabulated for the ANOVA analysis. Using Microsoft Excel, a "Two-Way ANOVA (without replication)" was performed to

either accept or reject the null hypothesis. The results of ANOVA analysis are shown in Table 4.

Since $|F_{Calculated}|$ (Rows) < $F_{critical}$ (Rows), the decision rule is that we fail to reject the null hypothesis (H_{n1}) and, hence, accept the null hypothesis (H_{n1}). This implies that there is no significant difference (significance level, $\alpha = 0.05$) in the mean peak PL intensities due to change in the angle of incidence in Sample B.

Since $|F_{Calculated}|$ (Columns) > $F_{critical}$ (Columns), the decision rule is to reject the null hypothesis (H_{n2}) and, hence, accept the alternate hypothesis (H_{a2}). This implies that there is a significant difference (significance level, $\alpha = 0.05$) in the mean peak PL intensities due to different metal coatings on Sample B.

Table 3: ANOVA of Sample B

Source of Variation	*SS*	*Degree of Freedom*	*MS*	*F*	*F crit*
Rows	556641588	4	139160396.9	2.997535964	3.259160053
Columns	1606538106	3	535512702.1	11.53502447	3.490299605
Error	557099159	12	46424929.88		
Total	2720278853	19			

ANOVA on Sample C:

A similar statistical analysis was conducted on readings obtained for Sample C. The results of the ANOVA analysis are shown in Table 5.

Since $|F_{Calculated}|$ (Rows) > $F_{critical}$ (Rows), the decision rule is that we reject the null hypothesis (H_{n1}) and, hence, to accept the alternate hypothesis (H_{a1}). This implies that there is a significant difference (significance level, $\alpha = 0.05$) in the mean peak PL intensities due to change in the angle of incidence in Sample C.

Since $|F_{Calculated}|$ (Columns) > $F_{critical}$ (Columns), the decision rule is to reject the null hypothesis (H_{n2}) and, hence, accept the alternate hypothesis (H_{a2}). This implies that there is a significant difference (significance level, $\alpha = 0.05$) in the mean peak PL intensities due to different metal coatings on Sample C.

Table 3: ANOVA of Sample C

Source of Variation	*SS*	*Degree of Freedom*	*MS*	*F*	*F crit*
Rows	596880200.7	4	149220050.2	3.379185273	3.259160053
Columns	2480818808	3	826939602.5	18.72658616	3.490299605
Error	529903055.8	12	44158587.98		
Total	3607602064	19			

Conclusions

The SEM characterization carried out on all the samples did not show significant roughness. The AFM characterization performed on the samples showed surface features at atomic resolutions. Cluster formation was observed on gold- and aluminum-coated samples and a Z-scale roughness on the order of ~ 2nm was observed on all the samples. It can be concluded that surface plasmons can be effectively excited by introducing roughness in the sample. Since the roughness in all the samples was not uniform, the angle of resonant surface-plasmon enhancement in each sample could not be determined. A better enhancement can be observed if uniform periodic corrugations are fabricated on the sample instead of random roughness. A statistical analysis revealed a significant difference in the mean peak PL intensities due to different metal coatings. Except for sample C, changing the incidence angle did not play a significant role in inducing a significant change in mean peak PL intensity. Photons from the light emitter couple more to the surface plasmons if the bandgap of the former is close to the surface-plasmon resonant energy of a particular metal.

Acknowledgments

The authors are grateful to the editors of IJERI for their support in the development of this paper.

References

[1] James D. Meindl, Qiang Chen, Jeffrey A. Davis, *Limits of Silicon Nanoelectronics for Terascale Integration*, Science, Vol 293, pp. 2044-2049, Sep 14, 2001.

[2] Gordon E. Moore, *Cramming More Components onto Integrated Circuits*, Electronics, Volume 38, Number 8, April 19, 1965.

[3] 1999- International Technology Roadmap for Semiconductors Edition.

[4] Anatoly V. Zayats and Igor Ismolyaninov, *Near-field Photonics: Surface Plasmon Polaritons and Localized Surface Plasmons*, Journal of Optics A: Pure and Applied Optics 5(2003), pp. S16-S50, IOP Publishing Ltd, 2003.

[5] Motoichi Ohtsu, Kiyoshi Kobayashi, Tadashi Kawazoe, Suguru Sangu, Takashi Yatsui, *Nanophotonics: Design, Fabrication, and Operation of Nanometric Devices using Optical Near Fields*, IEEE Journal of Selected Topics in Quantum Electronics, Vol. 8, No. 4, pp. 839-851, July / August 2002.

[6] Stephen Wedge, and W.L.Barnes, *Surface Plasmon-Polariton Mediated Light Emission Through Thin Metal Films*, Optics Express, Vol 12, No. 16, pp. 3673-3685, August, 2004.

[7] William L. Barnes, Alain Dereux, and Thomas W. Ebbesen, *Surface Plasmon Subwavelength Optics*, Nature, Vol. 24, pp. 824-830, Nature Publishing Group, 2003.

[8] Ohtsu M (Ed), *Nanotechnology and Nano/atom Photonics by Optical Near Fields*, Proc. SPIE- Int. Soc. Opt. Engg., Vol 4416, pp. 1-13, 2001.

[9] M. Boroditsky, R. Vrijen, T. F. Krauss, R. Coccioli, R. Bhat, and E. Yablanovitch, *Spontaneous Emission Extraction and Purcell Enhancement from Thin-Film 2-D Photonic Crystals*, Journal of Lightwave technology, Vol. 17, pp. 2096-2112, 1999.

[10] Koichi Okamoto, Isamu Niki, Alexander Shvarster, Yukio Narukawa, Takashi Mukai, and Axel Scherer, *Surface-Plasmon-Enhanced Light Emitting Based on InGaN Quantum Wells*, NATURE, Vol 3, pp. 601-605, September 2004, Nature Publishing Group, 2004.

[11] T. W. Ebbessen, H. J. Lezec, H. F. Ghaemi, T. Thio, and P. A. Wolff, *Extraordinary Optical Transmission Through Sub-wavlength Hole Arrays*, Nature, Vol. 391, pp. 667, Nature Publishing Group, 1998.

[12] Mark A. Emanuel, *Metalorganic Chemical Vapor Deposition for the Heterostructure Hot Electron Diode*, Noyes Publications, NY, April 1, 1989.

[13] Donald M. Mattox, *Handbook of Physical Vapor Deposition (PVD) Processing- Film Formation, Adhesion, Surface Preparation and Contamination Control*, Noyes Publications, NJ, 1998.

[14] John D. Cutnell, Kenneth W. Johnson, *Physics*, Fifth Edition, John Wiley & Sons Publications, NY, 2001.

[15] Rhianna A. Riebau, *Photoluminescence Spectroscopy of Strained InGaAs/GaAs Structures*, Thesis dissertation, University of Maryland at Baltimore County, 2002.

[16] Lyman Ott, *An Introduction to Statistical Methods and Data Analysis*, 3rd edition, PWS-Kent Publishing Company, Boston, 1988.

Biographies

PADMAREKHA VEMURI graduated from the Electronics Engineering Technology program at the University of North Texas with a Master's degree. Her M.S thesis was a study of surface plasmons and the factors influencing their efficiency.

VIJAY VAIDYANATHAN is Associate Dean for Undergraduate Studies in the College of Engineering at the University of North Texas. He earned his B.S. degrees in Physics (1985) and Electronics Engineering Technology (1988) from the University of Mumbai, India. He earned his M.S. and Ph.D. degrees in Biomedical Engineering from Texas A&M University, College Station, Texas.

ARUP NEOGI is Professor of Physics at the University of North Texas. He received his M.S. degree (1988) in Applied Physics from R.D. University in India. He earned his Ph.D. degree (1992) in Physics from Vikram University in India. He obtained a Doctor of Engineering degree (1999) from Yamagata University in Japan.